Studies in Overhead Wire—Goubau Line Above Ground

JIRO CHIBA, MEMBER, IEEE

Abstract—**The transition theory which Kikuchi [1]–[6] proposed first was improved and expanded in the range of the Sommerfeld line above ground and even the Goubau line (*G* line) above ground. Then it was proved by the experiment with the aid of the *G* line.**

The solution for the electromagnetic field produced by an overhead wire is derived using Maxwell's equations and treating the situation as a boundary value problem. In particular, the integrals which are caused by the finite conductivity of the earth and which are responsible for the distribution of the fields in the neighborhood of the surface of the earth are evaluated by means of the saddle-point method. Based on the field theory described above, the primary transmission line constants of the *G* line above ground (*R*, *L*, *C*, and *G*) and the secondary transmission line constants ($\gamma_0 = \alpha_0 + j\beta_0$ and Z_0) were obtained, and then the equivalent circuit for the *G* line above ground was given. The behavior of the line from an engineering standpoint is now completely determined by the usual simple circuit theory. The transition of the *G* line from a ground return transmission line of a surface-wave transmission line was proved experimentally.

I. Introduction

IT IS well known that a Goubau line (*G* line) [7] of infinite length in free space is capable of guiding electromagnetic waves without attenuation due to radiation, as for example Sommerfeld's wire waves [8].

In practice, however, the *G* line is installed at a certain height above ground. We have a classic theory of the propagation of the electromagnetic waves along overhead wires developed by Carson and by Pollaczek as early as 1926 [9], [10]. However, at the present time when the applications are tending toward the higher frequency regions, their analysis is not applicable since it is restricted to lower frequencies. Recently, remarkable advances in the theoretical aspects have been achieved through the studies of Kikuchi [1]–[6] and Amamiya [11]. Kikuchi was the first to give the transition theory (from ground return transmission line to surface-wave transmission line) for the Sommerfeld line above ground.

In practical applications, electromagnetic interference due to leakage fields set some limitations on such installations, whence the relevant theory of propagation and interference is very important. Although the analyses developed in the publications cited above are correct in their own rights, there is one aspect which has not been fully solved, namely, the correct evaluation of integrals ascribed to the finite conductivity of the earth.

Although a few works giving rigorous treatment in the complex domain have been published [12], no complete evaluations of such problems as the discontinuities due to the poles of integrands have been presented. Some of the results from our continued works have been published elsewhere [13]. We can say that great interest is focused on the earth's problem. Various authors (Wise [14], Sunde [15], Wait [16], Coleman [17], and Knyazev [18]) have studied the earth's problems, and recent research in this area has been promising (Wait [19]–[21], Dos Santos [22], Olsen and Chang [21], [23]). The objectives of the present paper are to evaluate the integrals due to the finite conductivity of the earth, utilizing the saddle-point method, to derive expressions for the electromagnetic fields produced by the transmission line of infinite length installed above ground, to find the primary constants of the *G* line *R*,*L*,*C*,*G* and the secondary constants Z_0,α,β,γ_0, and to prove the transition theory by experiment.

Manuscript received January 17, 1975; revised May 25, 1976.
The author is with the Department of Electrical Engineering, Tohoku University, Aoba Aramaki, Sendai, Japan.

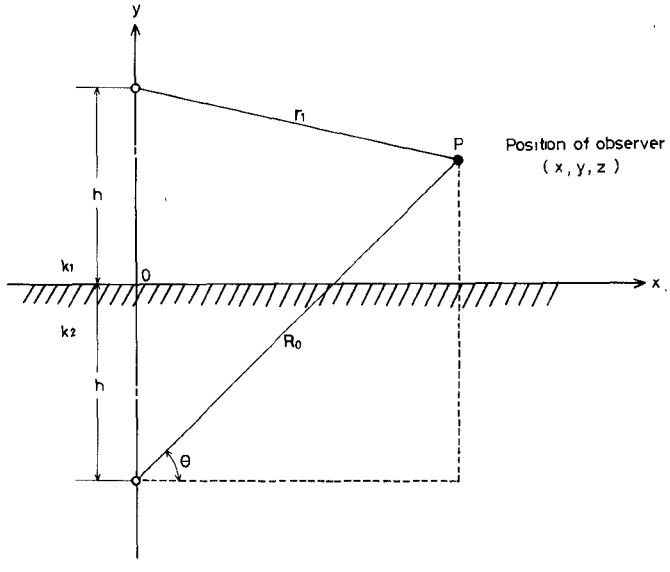

Fig. 1. The coordinate system.

II. Theoretical Formulation of Electromagnetic Fields

Assume that a line of infinite length and of sufficiently small diameter is installed at a height h above ground and carries a current $Ie^{-\gamma_0 z + j\omega t}$, ($I$ = total axial current in wire, γ_0 = propagation constant of the transmission line, ω = angular frequency = $2\pi f$, f = frequency). The diameter of the line is much smaller than h.

As shown in Fig. 1 in rectangular coordinates, the surface of the earth is the plane at $y = 0$. Beneath the surface or, in the region $y < 0$, the plane wave propagation constant is k_2 ($= \omega\sqrt{\mu_0\varepsilon_3(1 - j\sigma_2/\omega\varepsilon_2)}$, $\mathrm{Re}\, k_2 > 0$, $\mathrm{Im}\, k_2 < 0$,

μ_0 = permeability of free space, $\varepsilon_2 = \varepsilon_2{}^*\varepsilon_0$ = dielectric constant of the earth, σ_2 = conductivity of the earth, while above the surface, or in the region $y > 0$, the plane wave propagation constant is k_1 $(= \omega\sqrt{\mu_1\varepsilon_1} = \omega\sqrt{\mu_0\varepsilon_0})$.

From Maxwell's equations,

$$\boldsymbol{E} = \nabla\nabla \cdot \boldsymbol{\Pi} + k^2\boldsymbol{\Pi}$$

$$\boldsymbol{H} = j\omega\varepsilon\nabla \times \boldsymbol{\Pi} = \frac{jk^2}{\mu\omega}\nabla \times \boldsymbol{\Pi} \tag{1}$$

where $\boldsymbol{E},\boldsymbol{H}$ are the electric and magnetic fields. $\boldsymbol{\Pi}$ is the Hertzian vector given by [4], [20], [21]

$$\nabla^2\boldsymbol{\Pi}^{(1)} + k_1{}^2\boldsymbol{\Pi}^{(1)} = \frac{j\omega\mu_1}{k_1{}^2}\boldsymbol{J}, \qquad y > 0$$

$$\nabla^2\boldsymbol{\Pi}^{(2)} + k_2{}^2\boldsymbol{\Pi}^{(2)} = 0, \qquad y < 0$$

where

$$\boldsymbol{J} = I\boldsymbol{Z}\zeta\delta(x)\delta(y - h)$$

$\boldsymbol{Z}$ is the unit vector in the Z direction, and ζ stands for a coefficient required to establish the correspondence between the real wire current and the equivalent filament current.

The primary hertzian vector due to the line current consists exclusively of the z component of Π_{0z} where

$$\Pi_{0z} = \frac{\omega\mu_1 I\zeta}{4k_1{}^2}\frac{1}{\pi j}\int_{-\infty}^{\infty}\frac{e^{-jxu-|y-h|\sqrt{u^2-\lambda_1{}^2}}}{\sqrt{u^2-\lambda_1{}^2}}\,du \tag{2}$$

$$\lambda_1 = \sqrt{k_1{}^2 + \gamma_0{}^2} \tag{3}$$

$$\operatorname{Re}\sqrt{u^2 - \lambda_1{}^2} > 0$$

where we have used an appropriate Green's function as a particular integral of the inhomogeneous scalar Helmholtz equation.

The secondary field due to the earth consists of both the z and y components. If we introduce additional hertzian vectors Π_{I} and Π_{II} for the region $y > 0$ and $y < 0$, respectively, the resultant Hertzian vectors are

$$\Pi_z{}^{(1)} = \Pi_{0z} + \Pi_{\mathrm{I}z}, \qquad y \geq 0$$

$$\Pi_z{}^{(2)} = \Pi_{\mathrm{II}z}, \qquad y < 0 \tag{4}$$

$$\Pi_y{}^{(1)} = \Pi_{\mathrm{I}y}, \qquad y \geq 0$$

$$\Pi_y{}^{(2)} = \Pi_{\mathrm{II}y}, \qquad y < 0. \tag{5}$$

By matching fields at the boundary $y = 0$, we get

$$\Pi_z{}^{(1)} = A_1\left[H + \int_{-\infty}^{\infty} I_1 e^{-y\sqrt{u^2-\lambda_1{}^2}}\,du\right], \qquad y \geq 0$$

$$\Pi_z{}^{(2)} = A_2\int_{-\infty}^{\infty} I_1 e^{y\sqrt{u^2-\lambda_2{}^2}}\,du, \qquad y < 0 \tag{6}$$

$$\Pi_y{}^{(1)} = A_1\int_{-\infty}^{\infty} I_2 e^{-y\sqrt{u^2-\lambda_1{}^2}}\,du, \qquad y \geq 0$$

$$\Pi_y{}^{(2)} = A_2\int_{-\infty}^{\infty} I_2 e^{y\sqrt{u^2-\lambda_2{}^2}}\,du, \qquad y < 0 \tag{7}$$

where

$$A_1 = (\omega\mu_1 I\zeta)(4k_1{}^2)^{-1} \qquad A_2 = (\omega\mu_1 I\zeta)(4k_2{}^2)^{-1}$$

$$H = H_0{}^{(1)}(\lambda_1 r_1) - H_0{}^{(1)}(\lambda_1 R_0)$$

$H_0{}^{(1)}$ = Hankel function of the first kind of order zero, $\operatorname{Im}\lambda_1 > 0$

$$I_1 = 2(j\pi)^{-1}(\sqrt{u^2 - \lambda_1{}^2} - \sqrt{u^2 - \lambda_2{}^2}) \cdot (k_2{}^2 - k_1{}^2)^{-1}e^{-(jxu + h\sqrt{u^2-\lambda_1{}^2})}$$

$$I_2 = 2\gamma_0(j\pi)^{-1}(\sqrt{u^2 - \lambda_2{}^2} - \sqrt{u^2 - \lambda_1{}^2}) \cdot (N)^{-1}e^{-(jxu + h\sqrt{u^2-\lambda_1{}^2})}$$

$$N = k_2{}^2\sqrt{u^2 - \lambda_1{}^2} + k_1{}^2\sqrt{u^2 - \lambda_2{}^2},$$

$$\lambda_2 = \sqrt{k_2{}^2 - \gamma_0{}^2}, \quad \operatorname{Re}\sqrt{u^2 - \lambda_2{}^2} > 0$$

$$r_1 = \{x^2 + (y - h)^2\}^{1/2} \qquad R_0 = \{x^2 + (y + h)^2\}^{1/2}.$$

From (1), (6), and (7), E in the air is

$$E_x = A[C + S_1]$$

$$E_y = A[-D + S_2]$$

$$E_z = A[F + S_3 + S_4] \tag{8}$$

where

$$A = (\gamma_0 I\zeta)(j\omega\varepsilon_1\pi)^{-1}$$

$$C = (j\pi\lambda_1 x/4)\{(r_1)^{-1}H_1{}^{(1)}(\lambda_1 r_1) - (R_0)^{-1}H_1{}^{(1)}(\lambda_1 R_0)\}$$

$$D = (j\pi\lambda_1/4)\{(r_1)^{-1}(h - y)H_1{}^{(1)}(\lambda_1 r_1) + (R_0)^{-1}(h + y)H_1{}^{(1)}(\lambda_1 R_0)\}$$

$$F = (j\pi\lambda_1{}^2)(4\gamma_0)^{-1}\{H_0{}^{(1)}(\lambda_1 r_1) - H_0{}^{(1)}(\lambda_1 R_0)\}$$

$$S_1 = \int_{-\infty}^{\infty} juM\,du \qquad S_2 = \int_{-\infty}^{\infty}\sqrt{u^2 - \lambda_2{}^2}\,M\,du$$

$$S_3 = \int_{-\infty}^{\infty}\gamma_0 M\,du \qquad S_4 = \frac{k_1{}^2}{\gamma_0}\int_{-\infty}^{\infty} Q\,du \tag{9}$$

$$M = (k_1{}^2)(2N)^{-1}e^{-jxu-(y+h)\sqrt{u^2-\lambda_1{}^2}}$$

$$Q = \{2(k_2{}^2 - k_1{}^2)\}^{-1} \cdot (\sqrt{u^2 - \lambda_1{}^2} - \sqrt{u^2 - \lambda_2{}^2})e^{-jxu-(y+h)\sqrt{u^2-\lambda_1{}^2}}$$

where

$H_n{}^{(1)}$ Hankel function of the first kind of order n;
γ_0 $= \alpha_0 + j\beta_0$;
α_0 attenuation constant (nepers per meter);
β_0 phase constant (radians per meter).

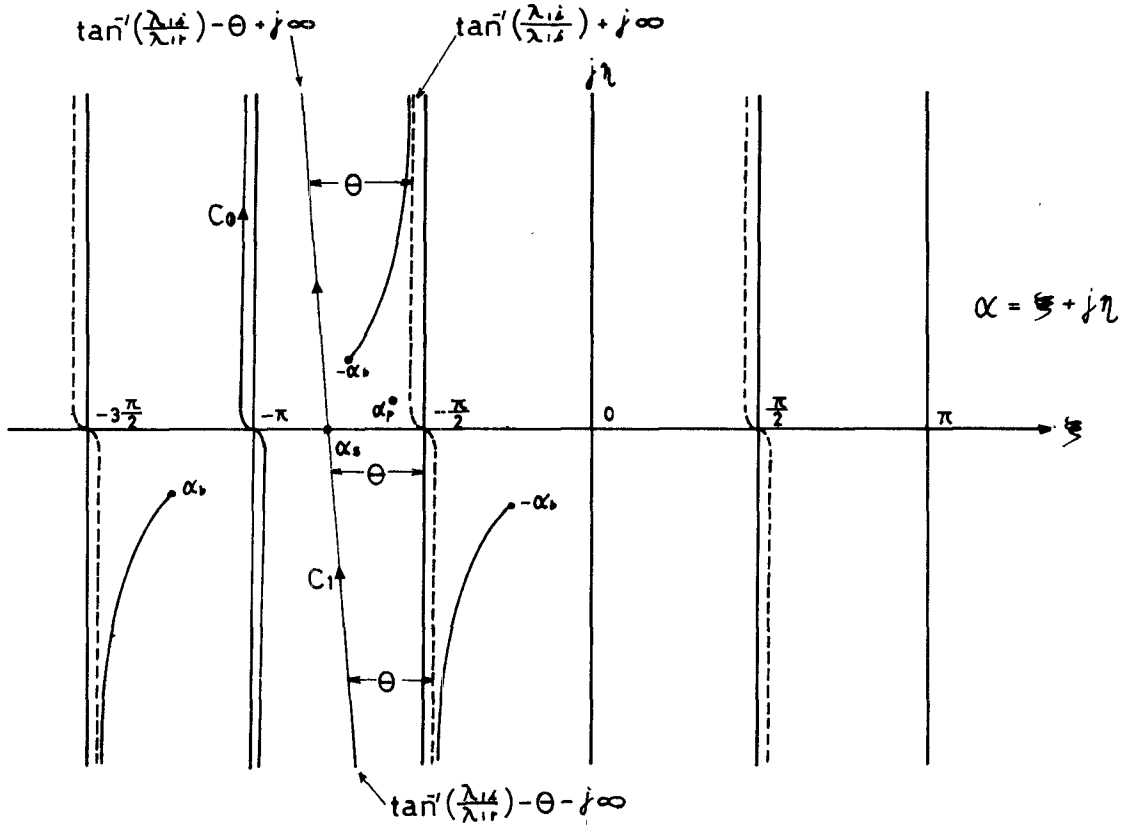

Fig. 2. Paths of integration in the α plane.

III. Evaluation of Integrals

A. Mapping of the Contour

Since the integrand involves four branch points, two in each half-plane ($u = \pm\lambda_1$ and $\pm\lambda_2$), a Riemann plane with four sheets is needed in order to derive a single-valued integrand.

In order to facilitate computation, we now transform the variable by introducing the following relation:

$$u = \lambda_1 \sin \alpha. \tag{10}$$

Furthermore, if we assume $\cos\theta = x/R_0$ and $\sin\theta = (y + h)/R_0$, S_1 in (9) will be reduced

$$S_1 = \frac{{k_1}^2}{2} \int_{C_0} \frac{j{\lambda_1}^2 \cos\alpha \sin\alpha}{N} e^{-j\lambda_1 R_0 \sin(\theta+\alpha)}\, d\alpha \tag{11}$$

where

$$N = jk_2{}^2\lambda_1 \cos\alpha + k_1{}^2\sqrt{{\lambda_1}^2 \sin^2\alpha - {\lambda_2}^2}.$$

Cuts and C_0 are as shown in Fig. 2.

As we are concerned with electromagnetic fields far away from the image of the line, the distance R_0 of the observer from the image of the line is very large so that we assume that $|\lambda_1|R_0 > 1$. With such values of R_0, the integral is dependent for the most part on the region near the saddle point. Hence the integration path C_0 is shifted to the line of steepest descent C_1 through the saddle point α_s, where

$$\alpha_s = (-\pi/2) - \theta. \tag{12}$$

Therefore, (11) is reduced to

$$S_1 = j\frac{{k_1}^2}{2} \int_{-\infty}^{\infty} \frac{{\lambda_1}^2 \cos\alpha \sin\alpha}{N} \cdot e^{j\lambda_1 R_0 + j(\lambda_1/2)R_0 S^2 \exp[j(\pi + (\lambda_{1r}/\lambda_{1i}))]} \cdot e^{j(1/2)(\pi+(\lambda_{1r}/\lambda_{1i}))}\, dS + K. \tag{13}$$

The additional term K is provided to take the residue into account which might appear by the passage across the pole when the contour is shifted from C_0 to C_1. Denoting the pole in α plane by α_p, we have

$$\sin\alpha_p = (\lambda_1)^{-1}\{{\lambda_1}^2 - (k_1{}^4)(k_1{}^2 + k_2{}^2)^{-1}\}^{1/2}$$

$$\cos\alpha_p = (\lambda_1)^{-1}(k_1{}^2 + k_2{}^2)^{-1/2}(-k_1{}^2).$$

Considering the values of k_1, k_2, and λ_1, this pole is near the $-\pi/2$ as shown in Fig. 2.

B. Integration along the Line of Steepest Descent and Computation of Residue

If it can be assumed that the term α involved in (13) is equal to α_s, we could readily perform the integration. The term, however, has been proved to be nearly equal to α_p. Hence we should avoid [24], [25] substituting α_s in $N(\alpha)$.

As an alternative, we develop $N(\alpha)$ as

$$N(\alpha) = N(\alpha_s) + \left(\frac{\partial N}{\partial \alpha}\right)_s (\alpha - \alpha_s). \tag{14}$$

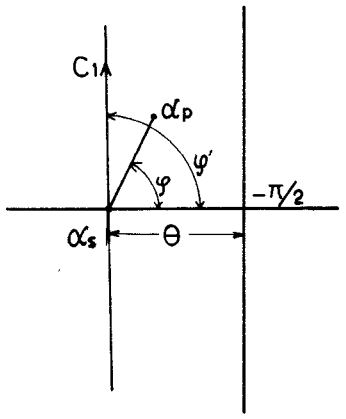

$$\alpha_p = \xi_p + j\eta_p \qquad \varphi' = \frac{1}{2}\left(\pi + \eta_p \frac{\lambda_{1r}}{\lambda_{1i}}\right)$$

Fig. 3. The value of ϕ with the pole across the C_1. If Im $T > 0$, then $\phi > \phi'$ and $K \neq 0$. If Im $T < 0$, then $\phi < \phi'$ and $K = 0$.

This value for $N(\alpha)$ introduced into (13) leads to

$$S_{1s} = \frac{k_1^2}{k_2^2}\lambda_1 \sin\theta \cdot e^{j\lambda_1 R_0 + j(1/2)\lambda_1 R_0 T^2}\sqrt{\pi} \cdot \left\{ j\frac{\sqrt{\pi}}{2} - \int_0^{T\sqrt{j(1/2)\lambda_1 R_0 \exp[j(\pi+(\lambda_{1r}/\lambda_{1i}))]}} \cdot e^{\lambda^2}\, d\lambda + K \right\}, \qquad \text{Im } T > 0 \text{ then } \phi > \phi'$$

$$= \frac{k_1^2}{k_2^2}\lambda_1 \sin\theta \cdot e^{j\lambda_1 R_0 + j(1/2)\lambda_1 R_0 T^2}\sqrt{\pi} \cdot \left\{ -j\frac{\sqrt{\pi}}{2} - \int_0^{T\sqrt{j(1/2)\lambda_1 R_0 \exp[j(\pi+(\lambda_{1r}/\lambda_{1i}))]}} \cdot e^{\lambda^2}\, d\lambda \right\}, \qquad \text{Im } T < 0 \text{ then } \phi < \phi' \quad (15)$$

where

$$T = \left\{ \tan\theta + \frac{k_1^2\lambda_1 \cos\theta}{2k_2^2\lambda_2} - \frac{k_1^2\lambda_1}{k_2^2\lambda_1 \cos\theta} \right\} \cdot e^{-j(1/2)(\pi+(\lambda_{1r}/\lambda_{1i}))}.$$

When $\theta < |\xi_p| - \frac{1}{2}\{\pi + \eta_p \cdot (\lambda_{1r}/\lambda_{1i})\}$, the pole across the C_1, then $\phi > \phi'$ (Fig. 3).

From (11),

$$K = -j\pi \frac{k_1^2}{k_2^2}\lambda_1 \sin\theta \cdot e^{j\lambda_1 R_0 + j(1/2)\lambda_1 R_0 T^2}. \quad (16)$$

The substitution of K thus obtained into the first part of (15) results in the same expression as the second part of (15).

When we introduce numerical distance $\rho = -\frac{1}{2}j\lambda_1 R_0 T^2$, we obtain

$$S_{1s} = -j\frac{k_1^2\lambda_1^2}{2} \frac{\sin\theta \cdot \cos\theta \cdot e^{j\lambda_1 R_0}}{k_2^2\lambda_1 \sin\theta + \frac{k_1^2\lambda_1^2}{2\lambda_2}\cos^2\theta - k_1^2\lambda_2} \cdot \sqrt{\frac{2\pi}{|j\lambda_1|R_0}}\{1 - V(\rho)\} \quad (17)$$

for both Im $T > 0$ and Im $T < 0$, where

$$V(\rho) = 1 - j\sqrt{\pi\rho}\cdot e^{-\rho}\,\text{erfc}\,(j\sqrt{\rho}) \sim -\left(\frac{1}{2}\cdot\frac{1}{\rho}\frac{1}{2}\cdot\frac{3}{2}\cdot\frac{1}{\rho^2} + \frac{1}{2}\cdot\frac{3}{2}\cdot\frac{5}{2}\cdot\frac{1}{\rho^3} + \cdots\right), \qquad |\rho| > 1$$

$$= 1 - j\sqrt{\pi\rho}\cdot e^{-\rho} - 2\rho \cdot \left(1 - \frac{2}{1\cdot 3}\rho - \frac{2\cdot 2}{1\cdot 3\cdot 5}\rho^2 - \cdots\right), \qquad |\rho| < 1. \quad (18)$$

Identical procedures apply to the integrals other than S_{1s}. In a practical surface-wave transmission line, we can assume $j\lambda_1 R_0 = -\lambda_{1i} R_0$.

Therefore, the final results are

$$S_{1s} = j\lambda_{1i} X \cos\theta \qquad S_{2s} = j\sqrt{\lambda_1^2\cos^2\theta - \lambda_2^2}\cdot X$$
$$S_{3s} = j\gamma_0 X \qquad S_{4s} = k_1^2(\gamma_0)^{-1} Y \quad (19)$$

where

$$X = (k_1^2\lambda_{1i}/2)\{(jk_2^2\lambda_{1i}\sin\theta) - (k_1^2\lambda_{1i}^2\cos\theta)(2\lambda_2)^{-1} - (k_1^2\lambda_2)\}^{-1} \cdot (\sin\theta)(2\pi/\lambda_{1i}R_0)^{1/2}\{1 - V(\rho)\}e^{-\lambda_{1i}R_0}$$

$$Y = (\lambda_{1i}/2)(k_2^2 - k_1^2)^{-1} \cdot \{(\lambda_{1i}\sin\theta - (\sqrt{\lambda_1^2\cos^2\theta - \lambda_2^2})\}(\sin\theta) \cdot (2\pi/\lambda_{1i}R_0)^{1/2}e^{-\lambda_{1i}R_0}.$$

On the line of steepest descent through the point α_b ($= \xi_b + j\eta_b$, refer to Fig. 4) [26], we obtain

$$S_{1b} = (-jk_1^4/k_2^2)(2R_0\sinh\eta_b)^{-1}(\pi/\lambda_{1i}\sinh\eta_b R_0)^{1/2} \cdot 2\sin\xi_b \cdot \cos\xi_b e^{-j\lambda_{1i}R_0(\cosh\eta_b + \sinh\eta_b)}. \quad (20)$$

The magnitudes obtained from (20) are negligibly smaller than those obtained from (19). The term's branch cut integral can be omitted.

IV. Determination of the Coefficient ζ

The ζ stands for a coefficient required to establish the correspondence between the real wire current (Sommerfeld line or G line) and the equivalent filament current. It is well known that in case of thin wire the coefficient $\zeta = 1$.

Electromagnetic wave propagation along a circular cylinder has been investigated in detail for a long time (for example, Sommerfeld [8], Stratton [27], and Goubau [7]) and the theories treat the Sommerfeld line without ground and the G line without ground.

The ζ in (8) is to be determined so that (8) matches those for the Sommerfeld line without ground or the G line without ground at $h = \infty$. When $h = \infty$ is introduced into (8) and (9), this leads to

$$H_0^{(1)}(\lambda_1 R_0) = H_1^{(1)}(\lambda_1 R_0) = 0$$
$$S_{1s} \sim S_{4s} = 0.$$

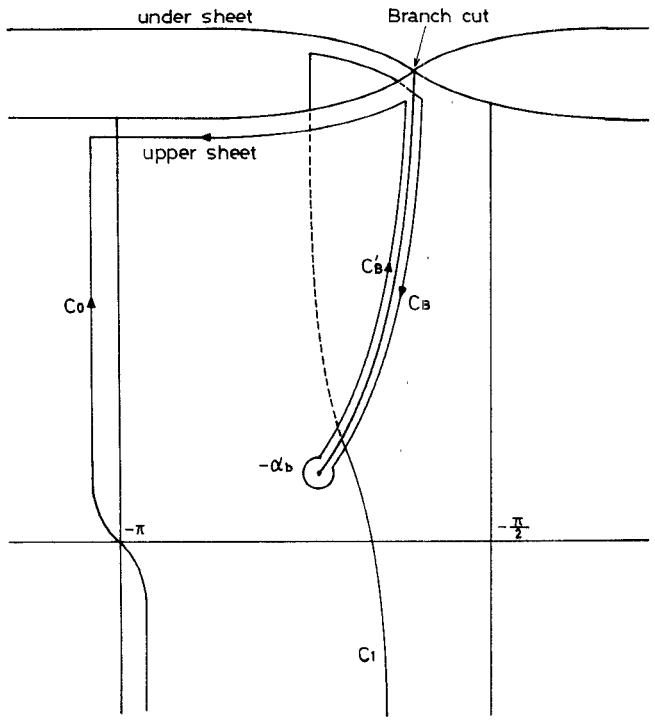

Fig. 4. Branch cut contour. $-\alpha_b = \xi_b + j\eta_b = \sin^{-1}(-\lambda_2/\lambda_1)$.

Thus from (8)

$$E_z = \frac{4\pi\varepsilon_1}{I{\lambda_1}^2}\,\zeta H_0^{(1)}(\lambda_1 r_1). \tag{21}$$

The filament current above ground is now reduced to the case of a filament current without ground.

On the other hand, E_z for the Sommerfeld line without ground is [8], [27]

$$E_z = \frac{I{\lambda_1}^2}{4\pi\varepsilon_1} H_0^{(1)}(\lambda_1 r_1) \tag{22}$$

and E_z for the G line without ground is [7], [27]

$$E_z = \frac{I{\lambda_1}^2}{4\pi\varepsilon_1}\left\{1 - \frac{(\lambda_d b)^2}{2}\ln\frac{2}{\gamma\lambda_d a}\right\} H_0^{(1)}(\lambda_1 r_1). \tag{23}$$

By comparing (21) with (22), $\zeta = 1$ for the Sommerfeld line, and by comparing (21) with (23)

$$\zeta = \left\{1 - \frac{(\lambda_d b)^2}{2}\ln\frac{2}{\zeta\lambda_d a}\right\}$$

for the G line, where

$$\lambda_d = \sqrt{\omega^2\mu_0\varepsilon_d + {\gamma_0}^2} \simeq \sqrt{\omega^2\mu_0\varepsilon_d - \beta^2} \tag{24}$$

$$\varepsilon_d = \varepsilon_0\varepsilon_d^*$$

ε_d^* specific inductive capacity of coated dielectric;
b radius of coated dielectric;
γ = 1.78107.

V. Series Impedance Z and Parallel Admittance Y of the G Line in the Presence of the Earth

A. Formulation for Z and Y

From Maxwell's equation,

$$E_{zt} = -\text{grad}\ \phi_c - j\omega A_{zt} \tag{25}$$

where E_{zt} is the Z component of the electric field at the wire surface ($x = 0, y = h - a$) ϕ_c and A_{zt} account for the scalar potential at the wire surface ($x = 0, y = h - a$) and for the z component of the vector potential at the wire surface ($x = 0, y = h - a$), and are represented by

$$\begin{aligned} \boldsymbol{A} &= \mu\varepsilon(\partial\boldsymbol{\Pi}/\partial t) \\ \phi &= -\nabla\cdot\boldsymbol{\Pi} \end{aligned} \tag{26}$$

given in part 2 of (6). We introduce the series impedance Z and the parallel admittance Y of the transmission line above the plane earth by the following equations:

$$\begin{aligned} Z &= \frac{1}{I\zeta}\left[E_{zt} + j\omega A_{zt}\right] \\ Y &= -\frac{\partial I\zeta}{\partial z}\frac{1}{\phi_c} = \frac{\gamma_0 I\zeta}{\phi_c} = \frac{\gamma_0 I\zeta}{\phi_a + \phi_{ab}}. \end{aligned} \tag{27}$$

ϕ_b is the scalar potential at the surface of the dielectric coated line ($r = b$). The following assumptions have been made in working out the theory of the transmission line: $a \ll h$, $b \ll h$, $a \ll$ wavelength, $b \ll$ wavelength. Under the aforementioned assumptions, E_{zt} and ϕ_{ab} are determined by only the primary field of the G line

$$\begin{aligned} E_{zt} &= \frac{(1+j)}{2\pi a\sqrt{2}}\, I\left\{1 - \frac{(\lambda_d b)^2}{2}\ln\frac{2}{\gamma\lambda_d a}\right\}\sqrt{\frac{\omega\mu_0}{\sigma_c}} \\ \phi_{ab} &= \frac{\gamma_0}{j\omega 2\pi\varepsilon_0}\, I\left\{1 - \frac{(\lambda_d b)^2}{2}\ln\frac{2}{\gamma\lambda_d a}\right\}\frac{\ln(b/a)}{\varepsilon_d^*(1 - j\tan\delta)} \end{aligned} \tag{28}$$

where σ_c is the conductivity of the wire. ϕ_b and $j\omega A_{zt}$ are obtained from (26) and (6)

$$\begin{aligned} j\omega A_{zt} = {} & \frac{j\omega\mu_0}{2\pi}\, I\left\{1 - \frac{(\lambda_d b)^2}{2}\ln\frac{2}{j\lambda_d a}\right\}\frac{j\pi}{2} \\ & \cdot \{H_0^{(1)}(\lambda_1 a) - H_0^{(1)}(\lambda_1 R_1)\} \\ & + \frac{j\omega\mu_0}{\pi}\, I\left\{1 - \frac{(\lambda_d b)^2}{2}\ln\frac{2}{\gamma\lambda_d a}\right\} \\ & \cdot \int_0^\infty \frac{e^{-R_1\sqrt{u^2-\lambda_1^2}}}{\sqrt{u^2-\lambda_1^2} + \sqrt{u^2-\lambda_2^2}}\, du \\ \phi_b = {} & \frac{\gamma_0}{j2\pi\omega\varepsilon_0}\, I\left\{1 - \frac{(\lambda_d b)^2}{2}\ln\frac{2}{\gamma\lambda_d a}\right\} \\ & \cdot \left[\frac{j\pi}{2}\{H_0^{(1)}(\lambda_1 b) - H_0^{(1)}(\lambda_1 R_1)\}\right. \\ & \left. + 2{k_1}^2\int_0^\infty \frac{e^{-R_1\sqrt{u^2-\lambda_1^2}}}{{k_2}^2\sqrt{u^2-\lambda_1^2} + {k_1}^2\sqrt{u^2-\lambda_2^2}}\, du\right] \end{aligned} \tag{29}$$

where $R = 2h - a$.

From (27)–(29),

$$\begin{aligned} Z = R + j\omega L = {} & \frac{(1+j)}{2\pi a\sqrt{2}}\sqrt{\frac{\omega\mu_0}{\sigma_c}} + \frac{j\omega\mu_0}{2\pi} \\ & \cdot\left[\frac{j\pi}{2}\{H_0^{(1)}(\lambda_1 a) - H_0^{(1)}(\lambda_1 R_1)\}\right] + \frac{j\omega\mu_0}{\pi}\, S_1 \end{aligned} \tag{30}$$

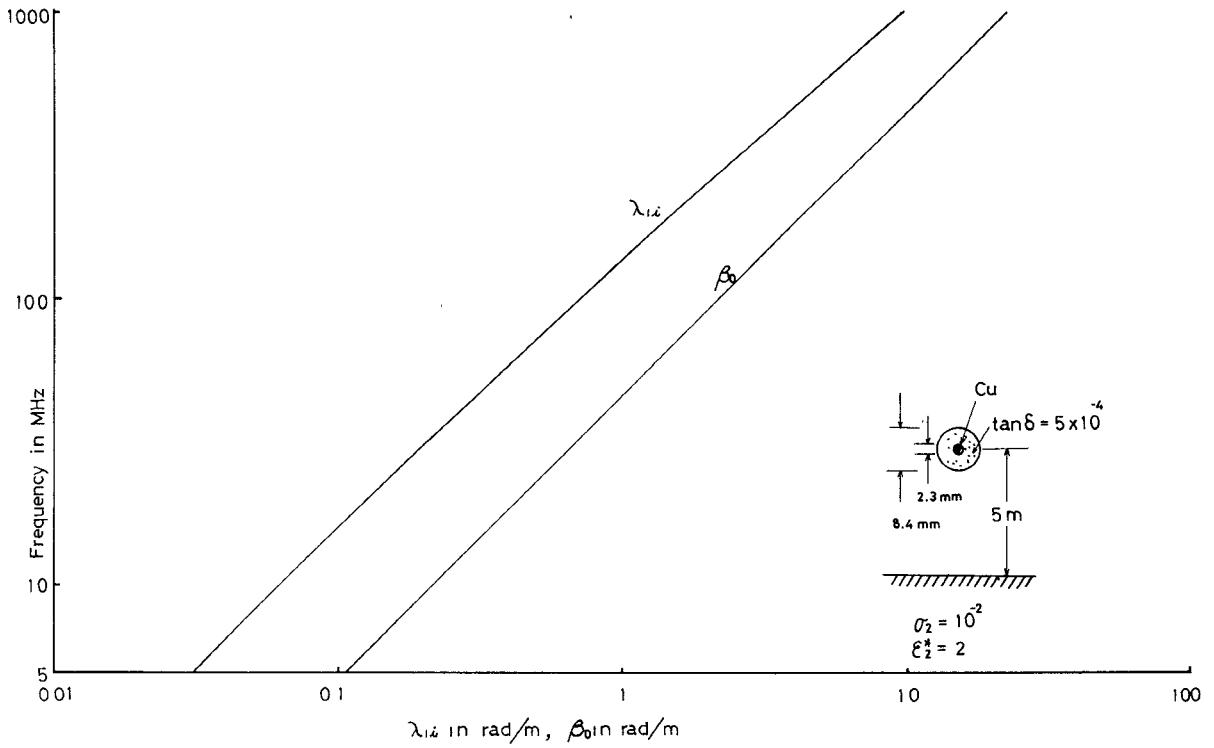

Fig. 5. The λ_{1i} and the β_0.

$$Y = G + j\omega C = \frac{j\omega 2\pi\varepsilon_0}{\dfrac{\ln (b/a)}{\varepsilon_d^*(1 - j\tan\delta)} + \dfrac{j\pi}{2}\{H_0^{(1)}(\lambda_1 b) - H_0^{(1)}(\lambda_1 R_1)\} + 2S_2} \tag{31}$$

where

$$S_1 = \int_0^\infty \frac{e^{-R_1\sqrt{u^2-\lambda_1^2}}}{\sqrt{u^2 - \lambda_1^2} + \sqrt{u^2 - \lambda_2^2}}\, du \tag{32}$$

$$S_2 = k_1^2 \int_0^\infty \frac{e^{-R_1\sqrt{u^2-\lambda_1^2}}}{k_2^2\sqrt{u^2 - \lambda_1^2} + k_1^2\sqrt{u^2 - \lambda_2^2}}\, du. \tag{33}$$

R, L, G, and C are series resistance, series inductance, parallel conductance, and parallel capacitance in the presence of the earth. The part $H_0^{(1)}(\lambda_1 R_1)$ stands for a contribution from the image of the line at $y = -h$. S_1 and S_2 are supplementary terms which take into account the effect of finite conductivity of the earth.

If $k_2 \to \infty$, $S_1 = S_2 \to 0$

and

if $h \to \infty$, $S_1 = S_2 \to 0$.

In much the same way as in Section III (saddle-point method), we obtain the simple results

$$S_1 = \frac{\lambda_{1i}}{\lambda_{1i} + \sqrt{\beta^2 - \omega^2\mu_0\varepsilon_2 + j\omega\mu_0\sigma_2}} \frac{1}{2}\sqrt{\frac{2\pi}{\lambda_{1i}R_1}}\, e^{-\lambda_{1i}R_1} \tag{34}$$

$$S_2 = \frac{\lambda_{1i}}{\lambda_{1i}\left(\varepsilon_2^* - j\dfrac{\sigma_2}{\omega\varepsilon_0}\right) - j\sqrt{\omega^2\mu_0\varepsilon_2 - \beta^2 - j\omega\mu_0\sigma_2}} \cdot \frac{1}{2}\sqrt{\frac{2\pi}{\lambda_{1i}R_1}}\, e^{-\lambda_{1i}R_1}. \tag{35}$$

Equations (34) and (35) are applicable to the region $\lambda_{1i}R_1 \geq 1$. In the case of the present paper, $R_1 \simeq 10$, and from Fig. 5 $\lambda_{1i} \simeq 0.1$ at 16 MHz. Therefore, (34) and (35) are applicable to the region frequency > 16 MHz.

Comparing the results of the numerical integration by a computer, the error committed in transmission loss is at most 7 percent even when $\lambda_{1i}R_1 = 1$ ($f = 16$ MHz, 17.5 dB/km—according to the results of the numerical integration; 18.9 dB/km—according to the results of the method of steepest descent).

VI. Characteristic Equation of the G Line Above Ground

From (25), (28), and (29), the characteristic equation is

$$\frac{\gamma_0}{\omega\varepsilon_0}\left[\frac{\ln (b/a)}{\varepsilon_d^*(1 - j\tan\delta)} + \frac{j\pi}{2}\{H_0^{(1)}(\lambda_1 b) - H_0^{(1)}(\lambda_1 R_1)\} + 2S_2\right] + \omega\mu_0\left[\frac{j\pi}{2}\{H_0^{(1)}(\lambda_1 a) - H_0^{(1)}(\lambda_1 R_1)\} + 2S_1\right] = j\frac{(1+j)}{a\sqrt{2}}\sqrt{\frac{\omega\mu_0}{\sigma_c}}. \tag{36}$$

In order to simplify the characteristic equation, we assume that a wire is a perfect conductor, $\lambda_1 = j\lambda_{1i}$ and $S_1 = S_2 = \tan\delta = 0$. Then the result is as follows:

$$k_1 = \frac{\lambda_{1i}}{\sqrt{\dfrac{K_0(\lambda_{1i}a) - K_0(\lambda_{1i}R_1)}{\{\ln(b/a)/\varepsilon_d^*\} + \{K_0(\lambda_{1i}b) - K_0(\lambda_{1i}R_1)\}} - 1}}. \tag{37}$$

This is in agreement with the result of Section VII [see (45)] according to circuit theory. Equation (37) holds to a very good approximation in the VHF and UHF regions. In Fig. 5 numerical results are given according to (37).

VII. Primary Transmission Line Constants of the G Line Above Ground

The following equations are applicable to the region $\lambda_{1i}R \geq 1$. From (30), (31), (34), (35) and the Hankel function formula,

$$\begin{aligned} R + j\omega L = Z = {} & \left\{\frac{(1+j)}{2\pi a\sqrt{2}}\sqrt{\frac{\omega\mu_0}{\sigma_c}}\right\} \\ & + \left\{\frac{j\omega\mu_0}{2\pi}[K_0(\lambda_{1i}a) - K_0(\lambda_{1i}R_1)]\right\} \\ & + \left\{\frac{j\omega\mu_0}{2\pi}\frac{\lambda_{1i}}{\lambda_{1i} + \sqrt{\beta^2 - \omega^2\mu_0\varepsilon_2 + j\omega\mu_0\sigma_2}} \right. \\ & \left. \cdot \sqrt{\frac{2\pi}{\lambda_{1i}R_1}}\, e^{-\lambda_{1i}R_1}\right\} \\ = {} & \{R_c^i + j\omega L_c^i\} + \{R_c^e + j\omega L_c^e\} \\ & + \{R_g + j\omega L_g^s\}(\Omega) \end{aligned} \tag{38}$$

where R_c^i, R_c^e, and R_g are the wire resistance and the equivalent resistance for the ground, respectively ($R = R_c^i + R_c^e + R_g$). L_c^i, L_c^e, and L_g^s are the wire internal inductance, the external inductance, and the equivalent series inductance for the ground, respectively ($L = L_c^i + L_c^e + L_g^s$). C_c and G_c are the wire capacitance and the wire leakage conductance, respectively ($Y_c = G_c + j\omega C_c$). C_d and G_d are the equivalent capacitance for the dielectric coat and the equivalent leakage conductance for the dielectric coat, respectively ($Y_d = G_d + j\omega C_d$). C_g, L_g^p, and G_g are the equivalent capacitance, the equivalent parallel inductance for the ground, and the equivalent leakage conductance for the ground, respectively ($Y_g = G_g + j(\omega C - (1/\omega L_g^p))$).

In Fig. 6 R, L, C, and G are indicated according to (38) and (39). In Fig. 7 the elements of R,L are indicated and in Fig. 8 the elements of C,G are indicated. From these relations [see (38) and (39)] the equivalent circuit of the G line above ground is as shown in Fig. 9.

VIII. Secondary Transmission Line Constants of the G Line Above Ground

By (38) and (39) the characteristic impedance Z_0 is

$$Z_0 = \sqrt{\frac{Z}{Y}} = \sqrt{\frac{R + j\omega L}{G + j\omega C}} \tag{40}$$

$$\doteqdot \sqrt{\frac{L}{C}} = 60\sqrt{\left\{\frac{\ln(b/a)}{\varepsilon_d^*} + K_0(\lambda_{1i}b) - K_0(\lambda_{1i}R_1)\right\}} \cdot \{K_0(\lambda_{1i}a) - K_0(\lambda_{1i}R_1)\}\ (\Omega). \tag{41}$$

Equation (41) holds to a very good approximation in the VHF and UHF regions. In Fig. 10 Z_0 is indicated [according to (41)].

$$\begin{aligned} G + j\omega C = Y = {} & \frac{j\omega 2\pi\varepsilon_0}{[K_0(\lambda_{1i}b) - K_0(\lambda_{1i}R_1)] + \left[\dfrac{\ln(b/a)}{\varepsilon_d^*(1 - j\tan\delta)}\right]} \\ & + \left[\frac{\lambda_{1i}}{\lambda_{1i}\left(\varepsilon_2^* - j\dfrac{\sigma_2}{\omega\varepsilon_0}\right) - j\sqrt{\omega^2\mu_0\varepsilon_2 - \beta^2 - j\omega\mu_0\sigma_2}}\sqrt{\frac{2\pi}{\lambda_1 R_1}}\, e^{-\lambda_{1i}R_1}\right] \\ = {} & \frac{1}{\dfrac{1}{\left\{\dfrac{j\omega 2\pi\varepsilon_0}{K_0(\lambda_{1i}b) - K_0(\lambda_{1i}R_1)}\right\}} + \dfrac{1}{\left\{\dfrac{j\omega 2\pi\varepsilon_0}{\dfrac{\ln(b/a)}{\varepsilon_d^*(1 - j\tan\delta)}}\right\}} + \dfrac{1}{\left\{\dfrac{j\omega 2\pi\varepsilon_0}{\dfrac{\lambda_{1i}\sqrt{2\pi/\lambda_{1i}R_1}\, e^{-\lambda_{1i}R_1}}{\lambda_{1i}\left(\varepsilon_2^* - j\dfrac{\sigma_2}{\omega\varepsilon_0}\right) - j\sqrt{\omega^2\mu_0\varepsilon_2 - \beta^2 - j\omega\mu_0\sigma_2}}}\right\}}} \\ = {} & \frac{1}{\dfrac{1}{G_c + j\omega C_c} + \dfrac{1}{G_d + j\omega C_d} + \dfrac{1}{G_g + j\left(\omega C_g - \dfrac{1}{\omega L_g^p}\right)}}\ (\mho/m) \end{aligned} \tag{39}$$

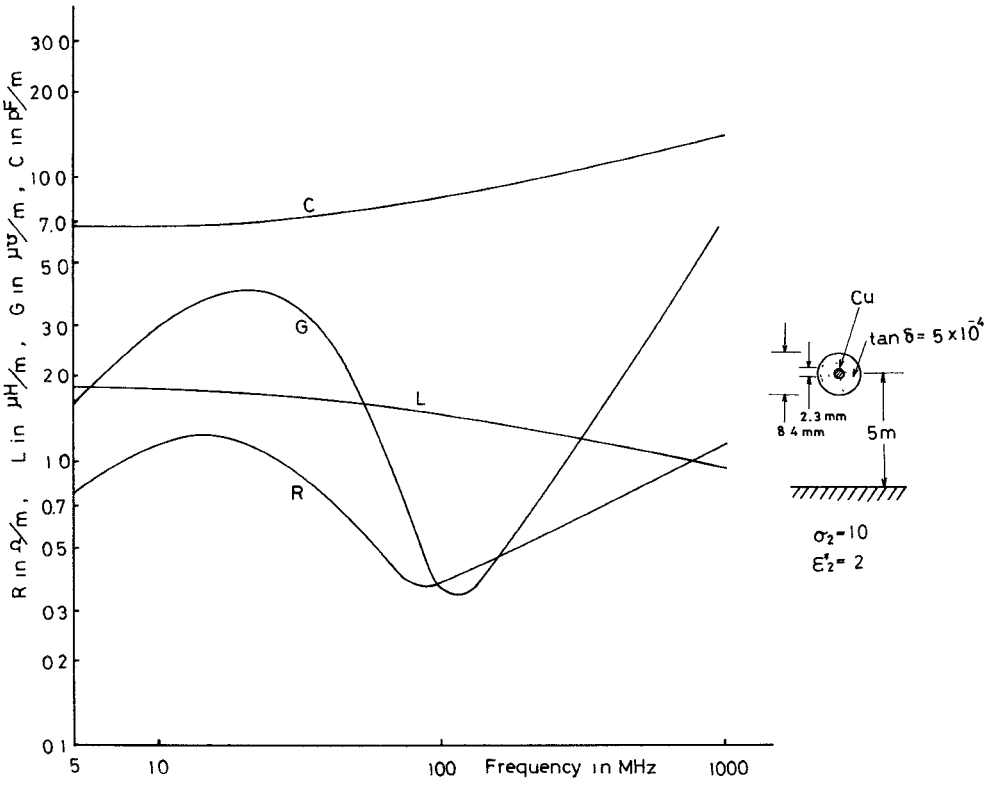

Fig. 6. Series resistance R, series inductance L, parallel capacitance C, and parallel conductance G of the G line above ground.

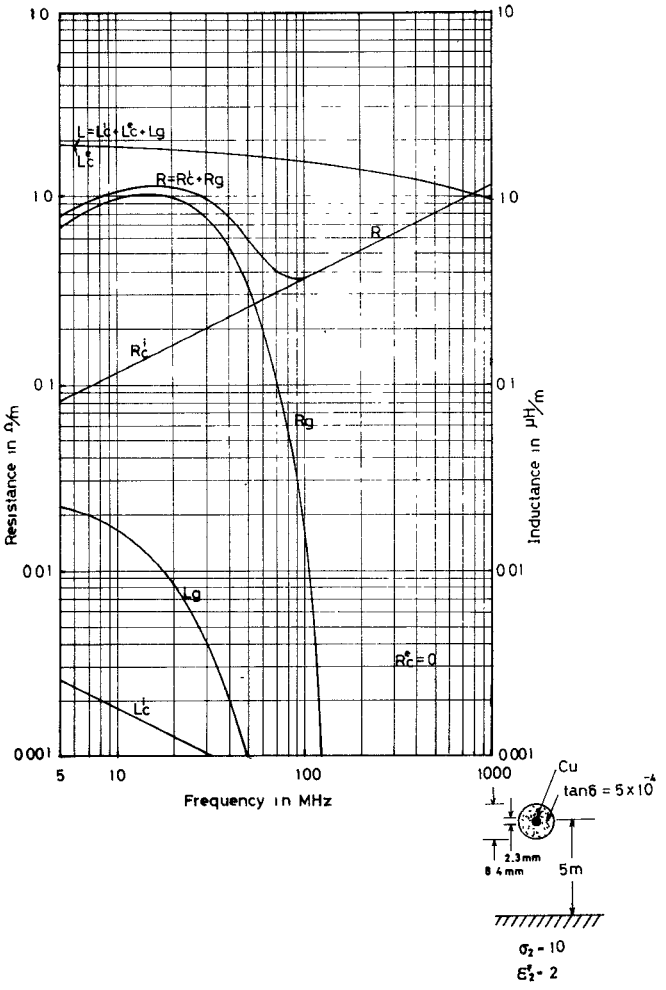

Fig. 7. The items of the series impedance Z ($Z = R + j\omega L = (R_c^i + R_c^e + R_g) + j\omega(L_c^i + L_c^e + L_g)$).

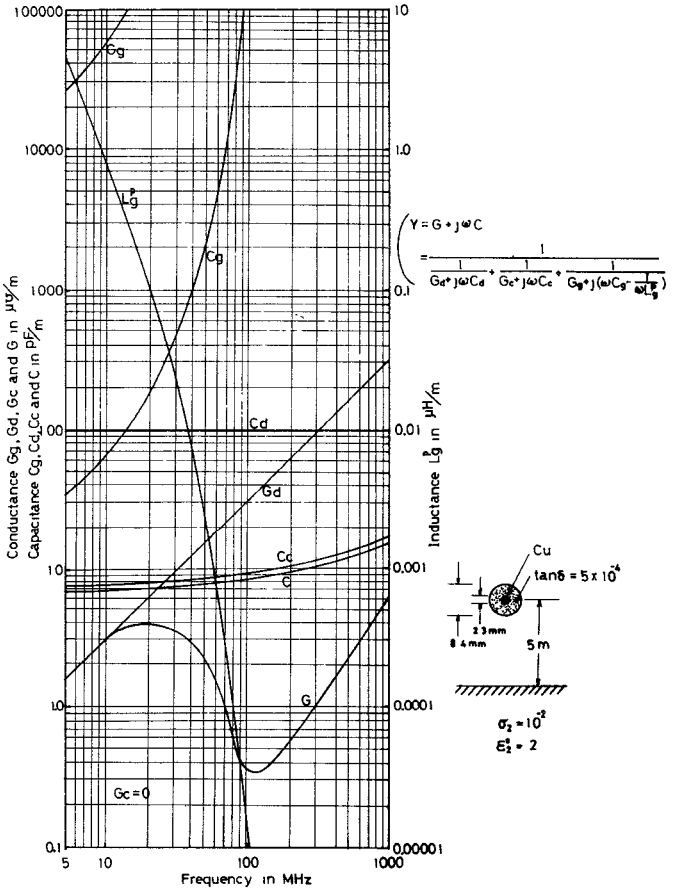

Fig. 8. The items of the parallel admittance Y.

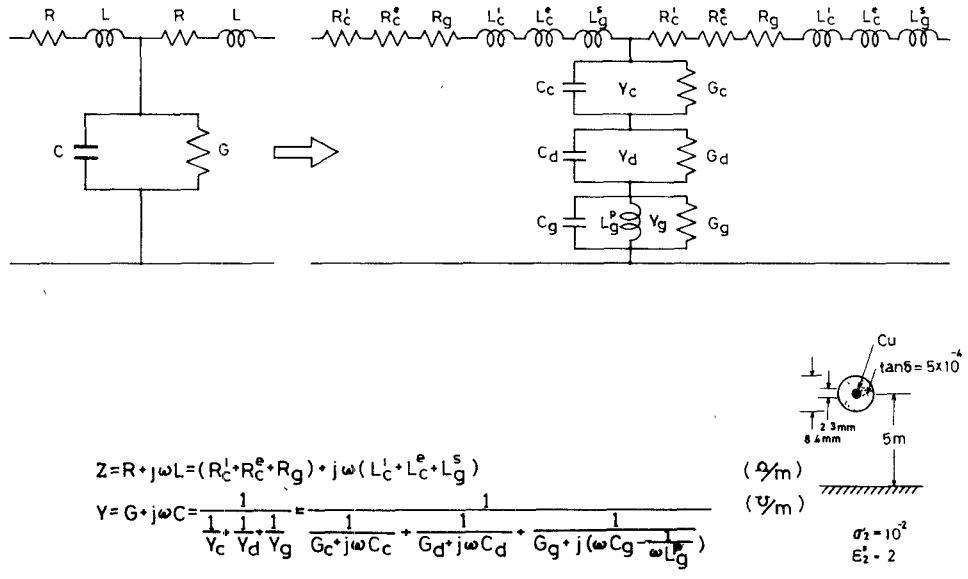

Fig. 9. Equivalent circuit of the G line above ground and items of the primary transmission line constants R, L, C, and G.

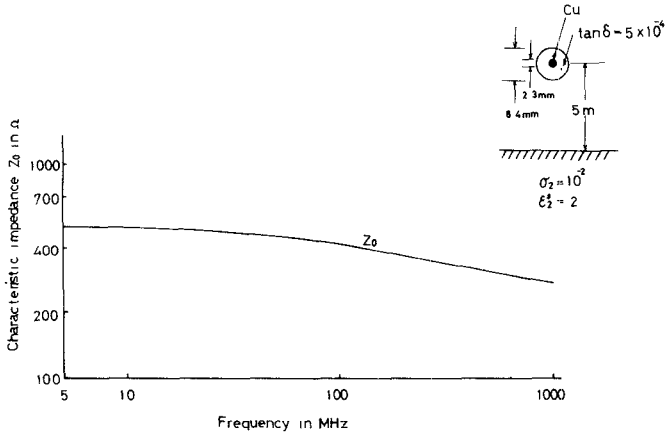

Fig. 10. Characteristic impedance of the G line above the ground.

By (38) and (39) the phase constant and the attenuation constant are

$$\gamma_0 = \alpha_0 + j\beta_0 = \sqrt{(R + j\omega L)(G + j\omega C)} = \sqrt{Z \cdot Y} \tag{42}$$

$$\alpha_0 = \frac{R}{2Z_0} + \frac{GZ_0}{2} \quad \text{(Np/m)} \tag{43}$$

$$\beta_0 = k_1 \sqrt{\frac{K_0(\lambda_{1i}a) - K_0(\lambda_{1i}R_1)}{\left\{\frac{\ln (b/a)}{\varepsilon_d^*}\right\} + \{K_0(\lambda_{1i}b) - K_0(\lambda_{1i}R_1)\}}} \quad \text{(rad/m)}. \tag{44}$$

From (44) and (3) the characteristic equation is

$$k_1 = \frac{\lambda_{1i}}{\sqrt{\dfrac{K_0(\lambda_{1i}a) - K_0(\lambda_{1i}R_1)}{\{\ln (b/a)/\varepsilon_d^*\} + \{K_0(\lambda_{1i}b) - K_0(\lambda_{1i}R_1)\}} - 1}}. \tag{45}$$

Equations (43) and (44) hold to a very good approximation in the VHF and UHF regions. This is shown in Fig. 5 [according to (44)].

In Fig. 11 α is indicated [according to (43)].

IX. Experimental Results

The experiment was carried out at the experimental installation set in the plane field. The outline of this installation is shown in Fig. 12. The measurement was by the Deschamps–Storer method.

A. The Deschamps–Storer Method [29]

In the Deschamps–Storer method, the total losses (G-line loss + two horn losses) are obtained from the measurement and an analysis of the scattering matrix; the G-line loss can be separated from the total losses by changing length of the G line.

An example of the measurement is shown in Fig. 11. Experimental values agree well with the theoretical results. The same is true of the results obtained by the standing wave method, but we omitted it from this paper. The transition theory was proved by the experiment.

Field distribution near the G line was obtained (close agreement between measured and calculated values was obtained), but we omitted it from this paper.

Conclusion

The features of the paper which seem to present new results are as follows:

1) presentation of a reasonable equivalent circuit as a passive line which involves the plane ground;
2) the extension of the theory to a dielectric-coated wire;
3) the saddle-point evaluation of the fields;
4) evaluation of transmission line parameters (R, L, C, G, Z_0, α_0, β_0, and γ_0) for the mode;
5) the verification of the transition theory which Kikuchi proposed first by experimental work.

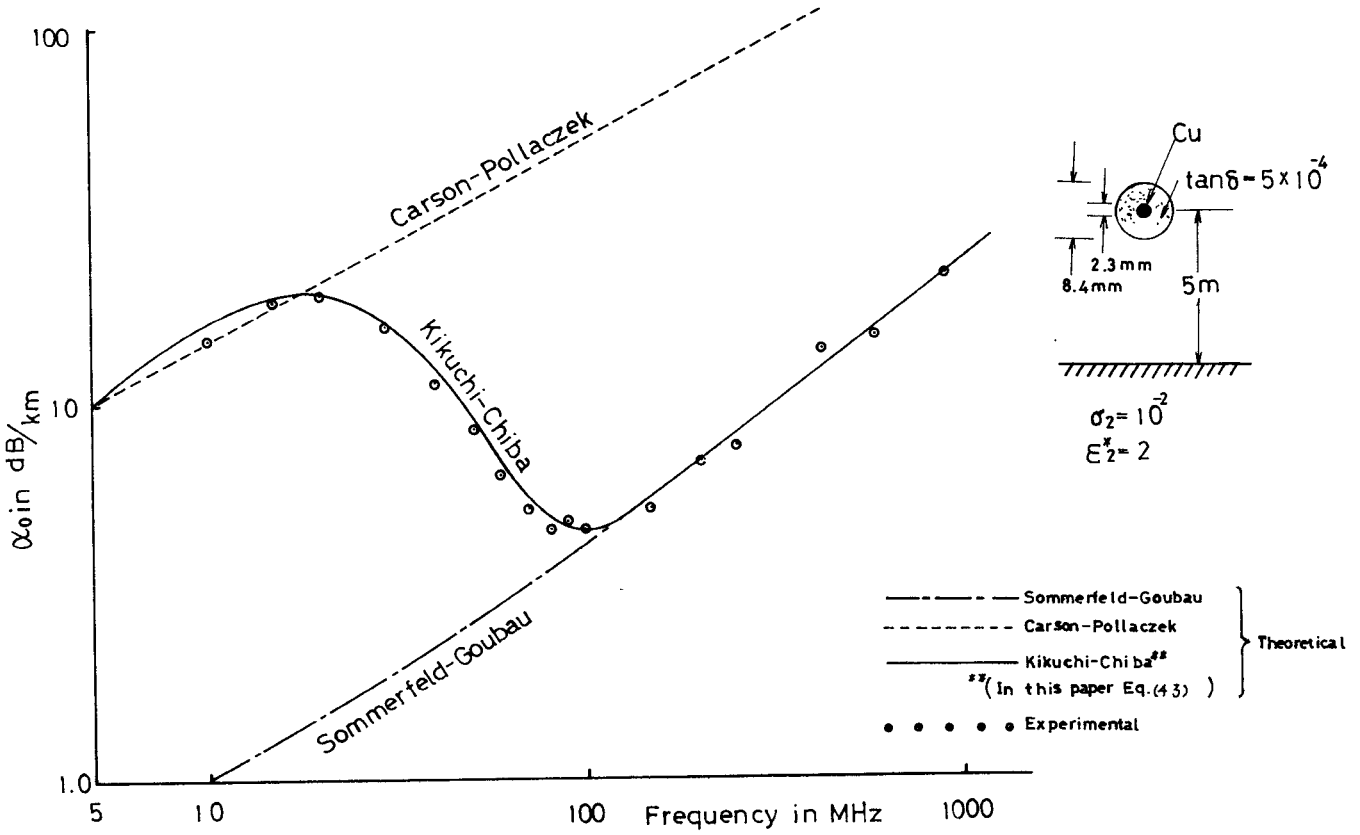

Fig. 11. Attenuation constant of the *G* line above ground. Ground return transmission line mode is transformed into surface-wave transmission line mode by elevation of frequency with a rise in degree of electromagnetic field concentration.

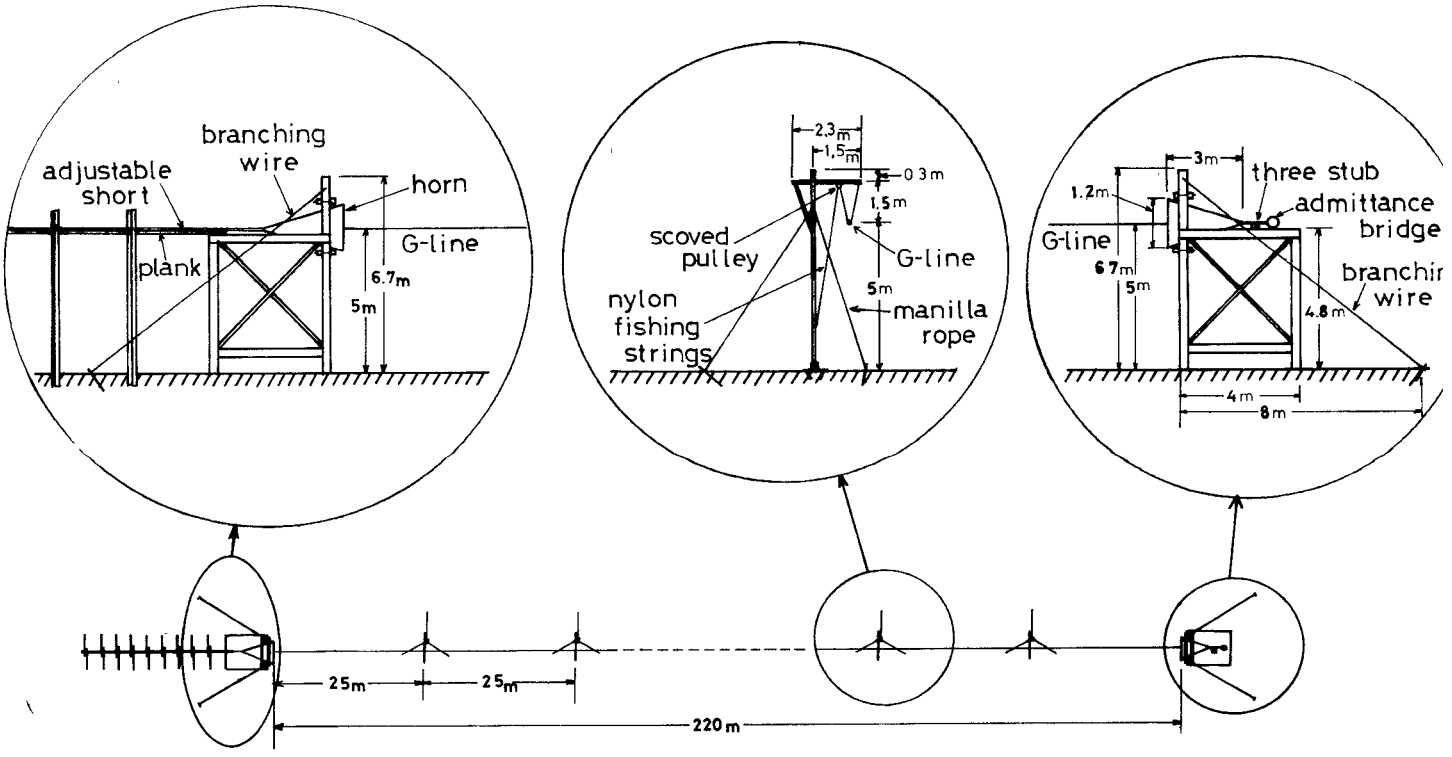

Fig. 12. Experimental installation.

Generally speaking, the surface-wave transmission line is influenced by the earth when it is wired over the earth. When frequency is low, it becomes the ordinary ground return transmission line mode; conversely, the ground return transmission line mode is transformed into the surface-wave transmission line mode by elevation of frequency with a rise in degree of electromagnetic field concentration. We need to consider the preceding characteristics in planning the applications of the overhead wire system.

Acknowledgment

The author wishes to acknowledge the dedicated guidance offered by Dr. R. Sato of Tohoku University. He also wishes to thank Dr. T. Nimura, Dr. Y. Mushiake, and Dr. S. Nishida for their helpful advice. The author wishes to express his gratitude to Dr. Kikuchi for many helpful discussions and suggestions during the course of this work. It is also his pleasure to acknowledge the hospitality of the members of his laboratory.

References

[1] H. Kikuchi, "On a ground return circuit at high frequencies," *J. Inst. Elec. Eng. Japan*, vol. 75, pp. 1176–1187, Oct. 1955.
[2] ——, "Wave propagation along infinite wire above ground at high frequencies," *Electrotech. J. Japan*, vol. 2, pp. 73–78, Dec. 1956.
[3] ——, "Wave propagation along an infinite wire above ground in the high frequency region on the transition from a ground return circuit to a surface waveguide," *Bull. Electrotech. Lab. Japan*, vol. 21, pp. 49–61, Jan. 1957.
[4] ——, "High-frequency electromagnetic fields around an infinite wire above plane earth," *J. IEE Japan*, vol. 77, pp. 61–73, June 1957.
[5] ——, "Electromagnetic fields on infinite wire above plane-earth at high frequencies," *J. Inst. Elec. Japan*, vol. 77, pp. 721–733, June 1957; also *Bull. Electrotech. Lab. Japan*, vol. 21, pp. 439–454, June 1957.
[6] ——, "Propagation coefficient of the Beverage aerial," *Proc. IEE* (London), vol. 120, pp. 637–638, June 1973.
[7] G. Goubau, "Surface waves and their application to transmission line," *J. Appl. Phys.*, vol. 21, pp. 1119–1128, Nov. 1950.
[8] A. Sommerfeld, "Über die Fortpflanzung electrodynamischer Wellen an einem zylindrischen Leiter," *Ann. Phys. u-Chemie*, vol. 67, pp. 233–290, 1899.
[9] J. Carson, "Wave propagation in overhead wires with ground return," *Bell Syst. Tech. J.*, vol. 5, pp. 539–554, Oct. 1926.
[10] F. Pollaczek, "Über das Feld einer unendlich langen wechselströmdurchflossenen Einfachleitung," *Elek. Nachr. Tech.*, vol. 3, pp. 339–359, Sept. 1926.
[11] Y. Amamiya, "On the field of a ground-return circuit in the medium-frequency region," *J. IEE Japan*, vol. 77, pp. 7–14, June 1957.
[12] K. Nagai, R. Sato, and J. Chiba: "Electromagnetic field produced by a surface-wave transmission line over flat earth and theoretical formulation of the modes of transmission," presented at the Dec. 1960 Tohoku Univ. Transmission Eng. Conf. Dec. 9, 1960.
[13] J. Chiba, R. Sato, and K. Nagai, "Leakage electromagnetic fields from surface wave transmission line," in *Proc. Joint Conv. Record of Elect. Comm. Engrs. of Japan*, p. 323, 1963.
[14] W. H. Wise, "Propagation of high-frequency currents in ground return circuits," *Proc. Inst. Radio Eng.*, vol. 22, pp. 522–527, Apr. 1934.
[15] E. Sunde, *Earth Conductance Effects in Transmission Line Systems*. New York: Van Nostrand, 1949, ch. 1–5, pp. 1–168.
[16] J. R. Wait, *Electromagnetic Waves in Stratified Media*. New York: Pergamon, 1962, ch. 2, pp. 8–63.
[17] B. L. Coleman, "Propagation of electromagnetic disturbances along a thin wire in a horizontally stratified medium," *Phil. Mag. Ser. 7*, vol. 41, pp. 276–288, Mar. 1950.
[18] A. S. Knyazev, "Engineering computation of the resistance of line conductors taking into account the earth's influence," *Radiotechika*, vol. 15 (a), pp. 21–32, 1960.
[19] J. R. Wait, "On the impedance of a long wire suspended over the ground," *Proc. Inst. Elec. Eng.* (London), vol. 49 (10), p. 1576, 1961.
[20] ——, "Theory of wave propagation along a thin wire parallel to an interface," *Rad. Sc.*, vol. 7, pp. 675–679, June 1972.
[21] D. C. Chang and J. R. Wait, "ELF propagation along a horizontal wire located above or buried in the earth," *IEEE Trans. Commun.*, vol. COM-22, pp. 421–428, Apr. 1974.
[22] A. F. Dos Santos, "Electromagnetic wave propagation along a horizontal wire above ground," *Proc. IEE* (London), vol. 119, pp. 1103–1109, Aug. 1972.
[23] R. G. Olsen and D. C. Chang, "A new model representation of wave propagation on a horizontal wire above earth," *Elec. Letters, IEE* (London), Apr. 1974.
[24] Y. Nomura, "On the theory of propagation of electromagnetic waves over the isotropic plane earth," *J. Inst. Elect. Comm. Japan*, vol. 37, pp. 14–19, Mar. 1954.
[25] A. Banõs, *Dipole Radiation in the Presence of a Conducting Half-Space*. New York: Pergamon, 1966, p. 71.
[26] L. M. Brekhovskikh, *Waves in Layered Media*, available in English translation. New York: Academic Press, 1960, pp. 270–290.
[27] J. A. Stratton, *Electromagnetic Theory*. New York: McGraw-Hill, 1941, ch. 6, p. 361, ch. 9, pp. 524–533, ch. 9, pp. 546–549.
[28] F. Stephen *et al.*, "On the rate of attenuation of signals conducted along overhead wires," *IEEE Trans. Electromag. Compat.*, vol. EMC-17, pp. 129–132, Aug. 1975.
[29] J. E. Storer, L. S. Sheingold, and S. Stein, "A simple graphical analysis of a two-port waveguide junction," *Proc. IRE*, vol. 41, pp. 1004–1013, Aug. 1974.